Brain Functional Connectivity Networks do not Return to Resting-state During Control Trials in Block Design Experiments*

Jamal Esmaelpoor[1,2], Tommy Peng[1,2], Beth Jelfs[3], Maureen J. Shader[4], Colette M. McKay[1,2], and Darren Mao[1,2]

***Abstract*— Many studies on morphology analysis show that if short inter-stimulus intervals separate tasks, the hemodynamic response amplitude will return to the resting-state baseline before the subsequent stimulation onset; hence, responses to successive tasks do not overlap. Accordingly, popular brain imaging analysis techniques assume changes in hemodynamic response amplitude subside after a short time (around 15 seconds). However, whether this assumption holds when studying brain functional connectivity has yet to be investigated. This paper assesses whether or not the functional connectivity network in control trials returns to the resting-state functional connectivity network. Traditionally, control trials in block-design experiments are used to evaluate response morphology to no stimulus. We analyzed data from an event-related experiment with audio and visual stimuli and resting state. Our results showed that functional connectivity networks during control trials were more similar to that of tasks than resting-state networks. In other words, contrary to task-related changes in the hemodynamic amplitude, where responses settle after a short time, the brain's functional connectivity networks do not return to their intrinsic resting-state network in such short intervals.**

I. INTRODUCTION

The brain is very active, even without any extrinsic input or stimulation. This unstimulated activity is known as the resting-state condition. During the resting state, spontaneous hemodynamic fluctuations occur in the cerebral tissue. These fluctuations have been shown to contain much information which can be used to detect brain disorders or evaluate brain performance [1]. When presented with a task, neural activations change in response to the task, which causes changes in cerebral blood flow. Many studies show that the brain's hemodynamic response amplitude returns to the resting state baseline after a short delay (around 15 seconds) [2], [3]. Accordingly, prevalent techniques for analyzing brain imaging data, such as general-linear modeling (GLM) [2] or psychophysiological interactions (PPI) [4], assume the perturbations in the amplitude of the hemodynamic waveform due to a task subside after a short delay (around 15 seconds). Therefore, in task-based studies, short inter-stimulus intervals (ISIs) are used between tasks to allow the hemodynamic amplitude to return to baseline [3], [5].

While using short ISIs for task-based studies in conjunction with morphological analysis of waveforms is well understood, in recent years, there has been increased interest in using connectivity measures to assess the same task-based studies. However, despite this increased interest, there needs to be more research on whether the same experimental design is valid for such measures. For example, functional connectivity (FC) describes the statistical dependencies between neurophysiological events in different brain regions. Much evidence indicates that task-based and resting-state functional brain networks are closely related, and the intrinsic resting-state network primarily determines functional brain networks during tasks [5], [6]. Nonetheless, the functional brain network cannot instantaneously switch between task states and the resting state, [7], and it needs to be clarified if it returns to the resting state network in the same timeframe as the amplitude of the waveforms.

In this paper, we assess the suitability of the current block-based experimental design for FC analysis. This is achieved by evaluating whether the brain functional network in control trials, where the subject is presented with no stimuli, relates more closely to the resting state network or the brain functional networks during a task. Our results provide insight into the brain connectivity network dynamics and how fast it returns to its intrinsic resting-state condition after a perturbation. The results are also crucial for assessing resting-state recording reproducibility by providing more insight into the influence of tasks on the resting state.

II. METHODS

A. Data Acquisition

Five adults (aged 23 to 72) participated in the experiment, four with normal hearing and one with severe hearing loss (the participant had a cochlear implant in one ear and a hearing aid in the other ear). This study was approved by the ethical standards of the Royal Victorian Eye and Ear Hospital human ethics committee, and all participants provided written informed consent. Full details of the experimental protocol and detailed results for morphology analysis can be found in [3]. Here we provide a brief summary of the experiment.

Functional near-infrared spectroscopy (fNIRS) was used for brain imaging as it is a low-cost recording technique

*This study was supported by a grant from the National Health and Medical Research Council of Australia to Colette M. McKay and Melbourne Research Scholarship to Jamal Esmaelpoor.

[1]J. Esmaelpoor, T. Peng, C.M. McKay and D. Mao are with The Bionics Institute, Melbourne, Australia {jesmaelpoor, tpeng, cmckay, dmao}@bionicsinstitute.org

[2]J. Esmaelpoor, T. Peng, C.M. McKay and D. Mao are with Department of Medical Bionics, University of Melbourne, Melbourne, Australia

[3]B. Jelfs is with Department of Electronic, Electrical and Systems Engineering, University of Birmingham, Birmingham, UK. b.jelfs@bham.ac.uk

[4]M.J. Shader is with Department of Speech, Language, and Hearing Sciences, Purdue University, West Lafayette, IN, USA mshader@purdue.edu

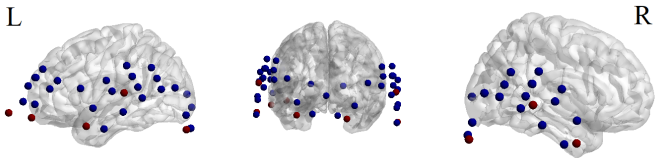

Fig. 1. The fNIRS recording montage included 44 long channels (blue circles) and eight short channels (red circles).

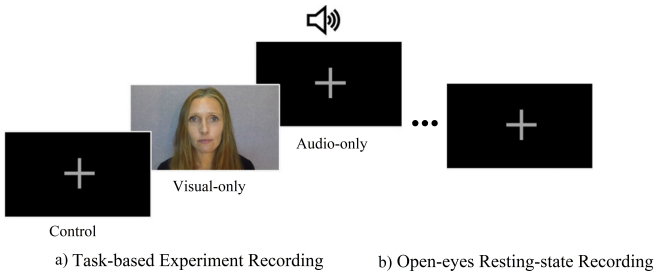

Fig. 2. Illustration of the experiment recordings: a) a task-based experiment telling a short children's story, including visual, audio, and control, b) a 5-minute open-eyes resting-state recording. (This figure is modified from [3].)

that measures changes in oxy- and de-oxyhemoglobin and, unlike fMRI, does not interfere with electronic devices, such as cochlear implants [3]. fNIRS is also less sensitive to patient motion and has a higher temporal resolution than fMRI [8], making it ideally suited to measuring hemodynamic responses during short periods. The experimental fNIRS montage, shown in Figure 1, comprised 44 long and eight short channels with approximately 35 and 7 mm distances between source and detector pairs, respectively. The montage covered the right and left auditory cortices, visual cortex, and inferior frontal gyrus.

The experiment consisted of two consecutive recordings (illustrated in Figure 2). First, the participants were asked to follow a short children's story told through 36 connected speech segments. For half of the segments, the participants saw a silent speaker (visual-only trials), and for the rest of the trials, they listened to the speaker with only a cross on the screen (audio-only trials). There were also ten control trials for which the participants watched the cross on the screen without audio or visual. The order of the trials was randomized, and trials were separated with an ISI of 15 to 30 seconds in which the cross was on the screen. The second recording was of a 5-minute open-eyes resting state while staring at the cross on the screen.

B. Preprocessing

Preprocessing was performed using MNE [9] and MNE-NIRS [10]. First, the raw recordings were converted to optical density. The scalp-coupling index (SCI) was used to measure channel quality [11], and channels with SCIs smaller than 0.5 were removed. Next, the temporal derivative distribution repair method was implemented on the remaining channels to remove motion artifacts [12]. The short channels measure systemic components in the blood flow; hence, they were used to regress these components out of the signals [13]. The optical signals were then converted to oxy- and de-oxyhemoglobin based on the modified Beer-Lambert Law [14]. As the final preprocessing step, a band-pass filter (0.033-0.40 Hz) was applied to remove low-frequency artifacts, such as Myer waves or baseline drifts, and high-frequency artifacts, e.g., heartbeats. The lower cut-off frequency was adjusted based on the duration of the trials ($\sim$15 seconds) and the approximate delay for the hemodynamic response to stimuli to settle. Accordingly, we chose a time window (w) of 30 seconds for each trial and adjusted the lower cut-off frequency of the filter to $1/w = 0.033$ Hz [15]. The data lengths for control trials and the resting-state recordings were almost the same (five minutes).

C. Functional Connectivity Analysis

For each subject, all of the trials from the same task (audio-only, visual-only, and control) were concatenated to create a timeseries for each one. Then, functional connectivity (FC) between pairs of channels was measured at each timeseries using Pearson correlation of the oxyhemoglobin concentration. Hence, we acquired four signed weighted connectivity matrices for each subject representing brain networks during audio-only, visual-only, and control trials and the open-eyes resting state. Having obtained the FC networks, the following analyses were performed to compare brain FC networks during control trials with the other connectivity networks and evaluate their differences and similarities.

1) Network-Based Statistics: Network-based statistics (NBS) were used to evaluate the differences between the brain networks obtained during control trials with the resting-state and task networks. NBS is a non-parametric technique to deal with the multiple-comparison problem when doing mass-univariate testing on the network edges. It relies on permutation testing to calculate the family-wise error rate (FWER)-corrected p-values of the connected components found in the mass-univariate comparison stage. In other words, NBS rejects the null hypothesis of no difference between graphs at the network level but not for individual edges [16]. So, we used NBS to determine subnetworks that our connectivity graphs were different at the network level.

2) Graph Laplacian Spectrum Analysis: The graph Laplacians of the networks were obtained by subtracting the network's adjacency matrix from the diagonal matrix of node strength, where each element on the diagonal equals the strength of the corresponding node. The normalized eigenvalue distribution of the graph Laplacian (known as the graph Laplacian spectrum) conveys crucial information about the network. For instance, the smallest eigenvalues and their corresponding eigenvectors can be used to define brain network modules. The smaller an eigenvalue is, the stronger its corresponding module is [17]. The peak amplitude of the spectrum is associated with the frequency of some specific motifs. For example, a peak around one indicates the frequency of nodes with similar connectivity profiles [17]. Hence, we compared the left tails and peaks of the graph

Laplacian spectrums of our networks to learn more about their similarities and differences.

3) Modularity Index: An alternative to the direct comparison of the connectivity matrices is to consider various nontrivial properties like centrality, modularity, and small-worldness that provide abstract features of networks [18]. Here, we compare our networks based on modularity, which is based upon the assumption brain nodes aggregate in densely connected modules, where nodes within modules are more strongly connected than between-module nodes [17]. Many studies show that tasks influence intrinsic (resting-state) FC networks and reduce modularity in the brain compared to resting state by strengthening the connections between modules [19], [20]. This dynamic reconfiguration of the FC network indicates interactions among different brain modules to accomplish a task. In this study, we calculated Newman and Girvan's modularity index (Q) [21] to compare the modularity of the brain FC networks during control trials with those of resting state and tasks. The measure is based on a divisive approach to defining hierarchical modules in the graph.

III. RESULTS

We calculated four connectivity matrices for each subject in different conditions. NBS was applied at $\alpha = 0.05$ significance level to compare different networks. Figure 3 indicates the sub-network, which was found to have significantly ($\rho = 0.03$) higher functional brain connectivity during control trials than resting state at group level. However, no significant difference (at $\alpha = 0.05$ level) was found between control-trial and task (visual or audio) networks. From Figure 3, we can see that most of the edges where control-trial and open-eyes resting-state networks differed either linked the two brain hemispheres or connected the inferior frontal gyrus to the rest of the brain covered by our montage. Therefore most of the links were inter-modular, and we could expect that brain modularity during control trials was lower than resting-state modularity. The following results support this expectation.

The Graph Laplacian analysis also revealed crucial differences between control-trial and resting-state networks. Figure 4 compares the eigenvalue distribution of the Laplacian matrices for different conditions. It also shows the eigenvalue distribution of corresponding random networks with preserved weight and strength distributions as defined in [22]. The results indicate that the brain graph Laplacian spectrums during control trials were more similar to task Laplacian spectrums than to the resting-state Laplacian spectrum. The resting-state networks had smaller eigenvalues than others, meaning the resting-state modularity index was higher than other networks. As expected, the left distribution tails for random networks were the shortest because their modularity indices were the smallest. Moreover, it is clear that the peak of the control-trial networks was more similar to those of task-based networks compared to resting state networks.

Table I compares the modularity indices of the networks for each subject. As the table shows, the modularity indices

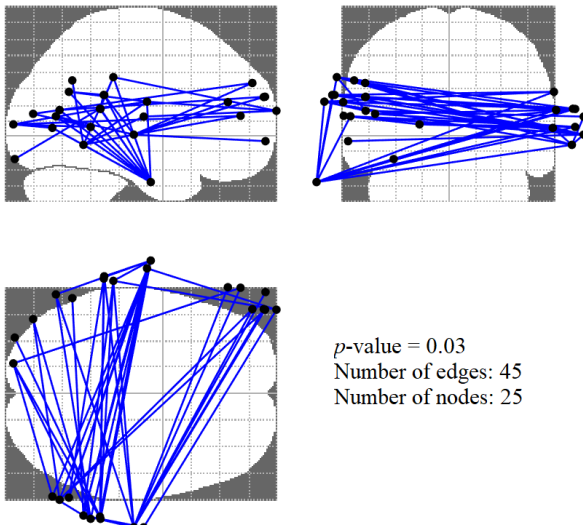

Fig. 3. Diagram of the sub-network identified by NBS where the functional connectivity during control trials at the group level was significantly higher than resting-state functional connectivity.

TABLE I

MODULARITY INDEX FOR DIFFERENT NETWORKS.

	Audio Net.	Visual Net.	Control Net.	Resting Net.
Subject 1	0.058	0.083	0.068	**0.210**
Subject 2	0.048	0.050	0.051	**0.067**
Subject 3	0.076	0.065	0.066	**0.302**
Subject 4	0.158	0.169	0.117	**0.280**
Subject 5	0.080	0.068	0.077	**0.110**

for all subjects during the resting state (shown in bold) were considerably higher than the control-trial networks'. In contrast, there was no significant difference in modularity for the control-trial networks and task graphs (the two-tailed p-values for paired t-tests comparing the modularity of audio and visual stimulation graphs with control-trial networks were 0.43 and 0.37, respectively.).

IV. CONCLUSIONS

This study investigated the brain response to task trials and control trials from the perspective of functional connectivity. Even though the conditions our participants underwent during the control trials and open-eyes resting state were similar (staring at a cross on the screen without audio or visual stimulations), our results revealed considerable differences between brain functional networks in these two situations. In contrast, the brain functional networks during control trials were more similar to task networks.

These results indicate that unlike the amplitude, which can be expected to have returned to baseline during control trials, the functional connectivity network has not returned to the intrinsic (resting-state) condition. This means the involvement of the brain's functional connectivity network in a task lasts longer than the time it experiences changes in the amplitude of the hemodynamic waveform.

We recommend that future works evaluate the importance of this mechanism for the brain to accomplish its work.

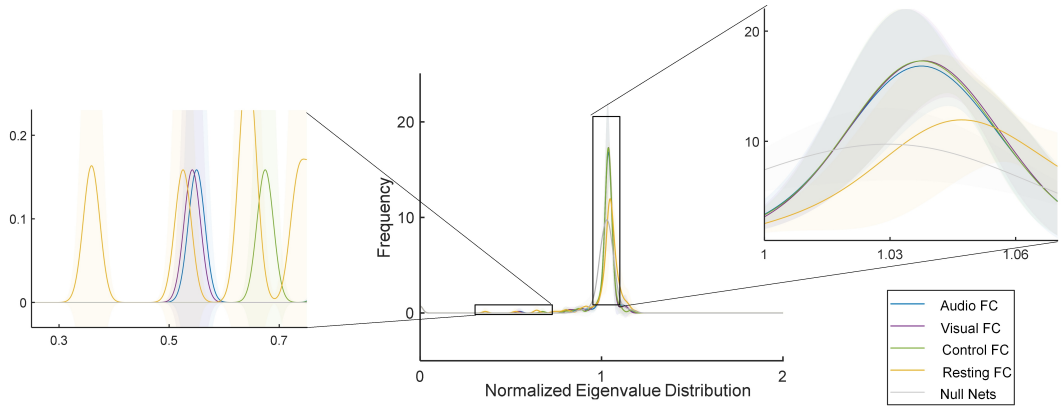

Fig. 4. Graph Laplacian spectrums of the four different conditions and the random null networks. On the left, the detailed view shows the left-tail distributions indicate resting-state networks have the smallest eigenvalues that correspond with the strongest modules. On the right, the detailed view again shows that the peaks of the spectrum for control networks were more similar to those of task-based networks compared to resting-state networks.

Moreover, when designing an experimental protocol for functional connectivity-based studies, ISIs sufficient for the brain hemodynamic response to settle down to baseline may be inadequate. Moreover, we recommend considering task-effect residuals on the resting-state functional connectivity when assessing its reproducibility.

ACKNOWLEDGMENT

The Bionics Institute acknowledges the support it receives from the Victorian Government through its Operational Infrastructure Support Program.

REFERENCES

[1] M. D. Fox and M. E. Raichle, "Spontaneous fluctuations in brain activity observed with functional magnetic resonance imaging," *Nat. Rev. Neurosci.*, vol. 8, no. 9, pp. 700–711, 2007.

[2] W. D. Penny, K. J. Friston, J. T. Ashburner, S. J. Kiebel, and T. E. Nichols, *Statistical parametric mapping: the analysis of functional brain images*. Elsevier, 2011.

[3] M. J. Shader, R. Luke, N. Gouailhardou, and C. M. McKay, "The use of broad vs restricted regions of interest in functional near-infrared spectroscopy for measuring cortical activation to auditory-only and visual-only speech," *Hear. Res.*, vol. 406, p. 108256, 2021.

[4] K. J. Friston, C. Buechel, G. R. Fink, J. Morris, E. Rolls, and R. J. Dolan, "Psychophysiological and modulatory interactions in neuroimaging," *Neuroimage*, vol. 6, no. 3, pp. 218–229, 1997.

[5] M. W. Cole, D. S. Bassett, J. D. Power, T. S. Braver, and S. E. Petersen, "Intrinsic and task-evoked network architectures of the human brain," *Neuron*, vol. 83, no. 1, pp. 238–251, 2014.

[6] M. Mennes, C. Kelly, S. Colcombe, F. X. Castellanos, and M. P. Milham, "The extrinsic and intrinsic functional architectures of the human brain are not equivalent," *Cereb. Cortex*, vol. 23, no. 1, pp. 223–229, 2013.

[7] Z. S. Saad, K. M. Ropella, R. W. Cox, and E. A. DeYoe, "Analysis and use of FMRI response delays," *Hum. Brain Mapp.*, vol. 13, no. 2, pp. 74–93, 2001.

[8] W.-L. Chen *et al.*, "Functional near-infrared spectroscopy and its clinical application in the field of neuroscience: advances and future directions," *Front. Neurosci.*, vol. 14, p. 724, 2020.

[9] A. Gramfort *et al.*, "MEG and EEG data analysis with MNE-Python," *Front. Neurosci.*, p. 267, 2013.

[10] R. Luke *et al.*, "Analysis methods for measuring passive auditory fNIRS responses generated by a block-design paradigm," *Neurophotonics*, vol. 8, no. 2, pp. 025 008–025 008, 2021.

[11] L. Pollonini, C. Olds, H. Abaya, H. Bortfeld, M. S. Beauchamp, and J. S. Oghalai, "Auditory cortex activation to natural speech and simulated cochlear implant speech measured with functional near-infrared spectroscopy," *Hear. Res.*, vol. 309, pp. 84–93, 2014.

[12] F. A. Fishburn, R. S. Ludlum, C. J. Vaidya, and A. V. Medvedev, "Temporal derivative distribution repair (TDDR): a motion correction method for fNIRS," *Neuroimage*, vol. 184, pp. 171–179, 2019.

[13] F. Scholkmann, A. J. Metz, and M. Wolf, "Measuring tissue hemodynamics and oxygenation by continuous-wave functional near-infrared spectroscopy—how robust are the different calculation methods against movement artifacts?" *Physiol. Meas.*, vol. 35, no. 4, p. 717, 2014.

[14] D. T. Delpy, M. Cope, P. van der Zee, S. Arridge, S. Wray, and J. Wyatt, "Estimation of optical pathlength through tissue from direct time of flight measurement," *Phys. Med. Bio.*, vol. 33, no. 12, p. 1433, 1988.

[15] N. Leonardi and D. Van De Ville, "On spurious and real fluctuations of dynamic functional connectivity during rest," *Neuroimage*, vol. 104, pp. 430–436, 2015.

[16] A. Zalesky, A. Fornito, and E. T. Bullmore, "Network-based statistic: identifying differences in brain networks," *Neuroimage*, vol. 53, no. 4, pp. 1197–1207, 2010.

[17] A. Fornito, A. Zalesky, and E. Bullmore, *Fundamentals of brain network analysis*. Academic press, 2016.

[18] E. Bullmore and O. Sporns, "Complex brain networks: graph theoretical analysis of structural and functional systems," *Nat. Rev. Neurosci.*, vol. 10, no. 3, pp. 186–198, 2009.

[19] M. G. Kitzbichler, R. N. A. Henson, M. L. Smith, P. J. Nathan, and E. T. Bullmore, "Cognitive effort drives workspace configuration of human brain functional networks," *J. Neurosci.*, vol. 31, no. 22, pp. 8259–8270, 2011.

[20] X. Wen *et al.*, "Reconfiguration of the brain functional network associated with visual task demands," *PLoS One*, vol. 10, no. 7, p. e0132518, 2015.

[21] M. E. J. Newman and M. Girvan, "Finding and evaluating community structure in networks," *Phys. Rev. E*, vol. 69, no. 2, p. 026113, 2004.

[22] M. Rubinov and O. Sporns, "Weight-conserving characterization of complex functional brain networks," *Neuroimage*, vol. 56, no. 4, pp. 2068–2079, 2011.